Airway IRF7^{hi} versus IRF7^{lo} molecular response patterns determine clinical phenotypes in children with acute wheezing

Siew-Kim Khoo, BSc (Hons)[1,2], James Read BSc (Hons)[2], Kimberley Franks, BSc (Hons)[1,2], Guicheng Zhang, PhD[1,4,5], Joelene Bizzintino, PhD[1,2], Laura Coleman, BSc (Hons)[1,2], Christopher McCrae, BSc (Hons)[6], Lisa Öberg, MSc[6], Niamh Troy, BSc (Hons)[2], Franciska Prastanti, MBBS[1,2], Janet Everard[1,2], Stephen Oo, MBBS, FRACP[3], Meredith L Borland, MBBS, FACEM[7,8], Rose A Maciewicz, PhD[6], Peter N Le Souëf, MD[2,3§], Ingrid A Laing, PhD[1,2§], Anthony Bosco, PhD[2§*].

[§] Joint senior authors

[*]Corresponding Author: Anthony.Bosco@telethonkids.org.au

Anthony Bosco

Telethon Kids Institute

100 Roberts Road

Subiaco 6008, Western Australia

Tel no.: +618 9489 7895

Fax no.: +618 9489 7700

Affiliations

[1] Division of Cardiovascular and Respiratory Sciences, The University of Western Australia, Perth, Western Australia, 6009, Australia.

[2] Telethon Kids Institute, The University of Western Australia, Perth, Western Australia, 6008, Australia.

[3] Division of Paediatrics, The University of Western Australia, Perth, Western Australia, 6009, Australia.

[4] School of Public Health, Curtin University, Perth, Western Australia, 6102, Australia.

[5] Centre for Genetic Origins of Health and Disease, The University of Western Australia and Curtin University, Perth, Western Australia, 6009 and 6102, Australia.

[6] Respiratory, Inflammation and Autoimmunity, Innovative Medicines & Early Development (IMED) Biotech Unit, AstraZeneca, Gothenburg, 431 50 Mölndal, Sweden.

[7] Emergency Department, Princess Margaret Hospital for Children, Perth, Western Australia, 6008, Australia.

[8] Divisions of Paediatrics and Emergency Medicine, School of Medicine, The University of Western Australia, Perth, Western Australia, 6009, Australia.

Summary

Asthma exacerbations are triggered by rhinovirus infections. We employed a systems biology approach to delineate upper airway gene network patterns underlying asthma exacerbation phenotypes in children. Cluster analysis unveiled distinct IRF7^{hi} versus IRF7^{lo} molecular phenotypes, the former exhibiting robust upregulation of Th1/type I interferon responses and the latter an alternative signature marked by upregulation of cytokine and growth factor signalling and downregulation of interferon gamma. The two phenotypes also produced distinct clinical phenotypes. For IRF7^{lo} versus IRF7^{hi}: symptom duration prior to hospital presentation was more than twice as long from initial symptoms ($p=0.011$) and nearly three times as long for cough ($p<0.001$); the odds ratio of admission to hospital was increased more than four-fold ($p=0.018$); and time to recurrence was shorter ($p=0.015$). In summary, our findings demonstrate that asthma exacerbations in children can be divided into IRF7^{hi} versus IRF7^{lo} phenotypes with associated differences in clinical phenotypes.

Key Words: Asthma, wheeze, rhinovirus, innate immunity, gene networks, gene expression profiling, systems biology.

Abbreviations

AHR, airway hyperresponsiveness; ARG1, Arginase 1, CSF3, Colony Stimulating Factor 3; CD38, Cluster of Differentiation 38; CD163, Cluster of Differentiation 163; cDCs, conventional (or myeloid) dendritic cells; DDX60, DExD/H-Box Helicase 60; ED, Emergency Department; EGF, Epidermal Growth Factor; ERK, Extracellular signal-Regulated Kinase; FCER1G, Fc Fragment Of IgE Receptor Ig; HMBS, Hydroxymethylbilane Synthase; IFNg, Interferon Gamma; IFNL1, Interferon Lambda 1; IL-1R2, Interleukin 1 Receptor Type 2; IRF7, Interferon Regulatory Factor 7; ISG15, Interferon-stimulated gene 15; MDA5, Melanoma

Differentiation-Associated protein 5; MX1, Myxovirus Resistance Protein 1; NAD, nicotinamide adenine dinucleotide; NCR1, Natural cytotoxicity triggering receptor 1; OSM, Oncostatin M; PD-L1, Programmed Death-Ligand 1; PPIA, Peptidylprolyl Isomerase A; PPIB Peptidylprolyl Isomerase B; RSAD2, Radical S-adenosyl methionine domain-containing protein 2; RSV, respiratory syncytial virus; RT-qPCR, quantitative reverse transcription PCR; RV, rhinovirus; sPLA2, secretory Phospholipase A2; TGFb, Transforming Growth Factor beta; THBS1, Thrombospondin 1; TNF, Tumor Necrosis Factor; TLR2, Toll-like Receptor 2.

Introduction

Exacerbations of asthma and wheeze are mostly triggered by respiratory viral infections and are one of the most common reasons for a child to seek emergency care.[1] Previous studies from our group have demonstrated that rhinovirus (RV) species C is the most frequent viral pathogen detected in children who present to the local emergency department (ED) with an asthma exacerbation.[2] However, the molecular mechanisms that determine susceptibility to RV and expression of respiratory symptoms are not well understood. Previous investigations of airway epithelial cells infected with RV *in vitro* found that type I and III interferon responses were deficient in adults with asthma, leading to impaired viral control and exaggerated secondary responses.[3, 4] However, this finding was replicated in some studies but not others.[5] Human adult asthmatic volunteers experimentally infected with RV *in vivo* have exaggerated IL-25 and IL-33 responses, which drive Th2 inflammation.[6, 7] Although these data provide a plausible mechanism to link RV infection with the pathogenesis of asthma, they are based on experimental models with artificial infections from laboratory RV strains. Hence, the extent they can recreate the complex environmental conditions underpinning natural RV-induced exacerbations is unclear.[1, 8] Indeed, studies of naturally occurring virus-induced exacerbations report increased rather than decreased interferon responses.[9-11] In this study, we have utilized an unbiased, systems biology approach to elucidate the innate immune mechanisms that are operating in the upper airways during natural exacerbations of asthma or wheezing in children.[9, 10] Our findings provide new insights into the role of gene networks, particularly IRF7, and their relationship to clinical phenotypes in this disease.

Results

Characteristics of the study population

The study was based on a case/control design. The cases (n=56) consisted of children who presented to the ED with an acute exacerbation of asthma or wheeze. The controls consisted of children who were either siblings of the cases, or they were recruited from the general community (controls, n=31). Convalescent samples (n=19) were available from children after they had recovered from an acute exacerbation of asthma or wheeze, but only a subset of these convalescent samples (n=5/19) were paired with acute samples. Samples from an independent group of children (n=99) with exacerbations of asthma or wheeze were utilised as a replication cohort. The characteristics of the study participants are presented in Table 1.

Children with wheezing exacerbations were younger (mean = 4.35 (SD 3.31) years) than controls (6.40 (SD 4.41) years, $p = 0.025$) and had fewer Caucasians (46.4% vs 78.6%, $p = 0.006$). A higher proportion of the children with wheezing exacerbations were sampled during winter, compared to convalescence ($p = 0.001$) and controls ($p = 0.028$). Respiratory virus, in particular, RV, was widely detected during wheezing exacerbations (87.0%, and 66.1%, respectively) compared with convalescence (42.1% and 26.3%, $p < 0.001$ and $p = 0.003$, respectively) and controls (58.1% and 32.3%, $p = 0.004$ and $p = 0.003$, respectively). RV-C was more prevalent during wheezing exacerbations (46.4%) compared with controls (12.9%, $p = 0.002$). The number of viruses detected during acute exacerbations (1.13 (SD 0.76) was higher than during convalescence (0.47 (SD 0.61), $p = 0.001$). No difference in bacterial detection was observed between the groups.

The proportion of children with wheezing exacerbations recruited in winter in the replication cohort was lower than the discovery cohort ($p < 0.001$, Table 1). The replication cohort was also more atopic (78.8% vs 60.7%, $p = 0.024$), and had lower detection rates of respiratory viral and bacterial pathogens compared to the latter. Respiratory symptoms, hospital admissions and medication usage were not different in the discovery and replication cohorts.

Gene expression profiling of exacerbation responses in the upper airways

Nasal swab specimens were collected from the children and gene expression patterns were profiled on microarrays. Cellular composition data of the samples was not available, and therefore a computational approach was employed to estimate the proportions of different cell types directly from the microarray profiles.[31] As illustrated in Figure 1a, the highest proportions were observed for neutrophils, epithelial cells, and monocytes. Stratification of the subjects by case/control status and RV detection revealed that wheezing exacerbations were associated with increased proportions of M1 macrophages and decreased proportions of conventional dendritic cells (Figure 1b). The proportions of the other cell types were mostly comparable across the groups. The relationship between case/control status, RV detection and cellular composition for each individual child is illustrated in Figure 1c.

To identify differentially expressed genes, we undertook group-wise comparisons employing *LIMMA* in combination with *Surrogate Variable Analysis*, which adjusts the analysis for all estimated sources of unwanted biological and technical variation (See Methods). Comparison of gene expression patterns between children with RV positive wheezing exacerbations (n=37) versus RV negative controls (n=21) revealed that 137 genes were upregulated and 82 genes were downregulated (adjusted p-value < 0.05, Table S1). Pathways analysis demonstrated that the upregulated genes were highly enriched for type I interferon signalling (adjusted p-value = 4.8×10^{-22}, relevant genes are highlighted in Table S1). Type I interferon signalling (adjusted p-value = 8.5×10^{-31}, Table S2) was also upregulated in children with RV positive exacerbations in comparison to RV negative convalescent children (n=14).

Gene expression patterns were then assessed in children with RV negative exacerbations. Comparison of these children (n=19) with RV negative controls (n=21) revealed that 17 genes were upregulated and 10 genes were downregulated (adjusted p-value < 0.05, Table S3). Similar results were obtained by comparing children with RV negative exacerbations versus RV negative convalescent children (n=14), where 30 differentially expressed genes were identified (adjusted p-value < 0.05, Table S4). While a subset of these genes were also

upregulated in children with RV positive exacerbations (e.g. IL-18R1, CD163), a notable difference was the lack of an interferon signature.

Discovery of molecular sub-phenotypes of acute wheezing illnesses

The findings above suggested that children with RV positive exacerbations mount an interferon response but there appears to be additional heterogeneity. As the data analysis strategy relied on group-wise comparisons (with LIMMA/SVA), this approach cannot shed any insight into subject-to-subject variations in gene expression patterns within each group. To obtain more detailed information in this regard, we employed hierarchical clustering (See Methods). To ensure that the clustering did not simply reflect variations in cellular composition (observed above in Figure 1), we utilised a set of negative control genes (i.e. genes not related to the outcome of interest) to model unwanted variation in the data, and removed these effects using regression (See Methods and Figure S1). This strategy preserves the gene expression signature associated with acute exacerbations in the data, and removes the strong correlation structure between samples that reflect variations in cellular composition (Figure S1). As illustrated in Figure 2a, cluster analysis of the corrected data divided the subjects into five distinct clusters or molecular phenotypes (labelled S1-S5). Likewise, the genes were also divided into five clusters labelled G1-G5. Notably, the majority of children with exacerbations (45/56 = 80%) were found within clusters S1 and S2, and there was no difference in RV detection between these cluster groups of children (RV detection rates for children with exacerbations in cluster S1 vs cluster S2 were 73% vs 58%, p-value = 0.347). The other three clusters S3-S5 contained the bulk of the controls and the convalescent samples, as well as 11 remaining children with exacerbations.

To examine the overall expression of each gene cluster across the children, principal component analysis was employed to summarise the expression data for each cluster, and the first principal component was plotted across the subjects, stratified into their respective clusters. This analysis revealed that the most striking difference between the subjects in cluster groups S1 and S2 was the differential expression of the set of genes in cluster G5 (Figure 2b), and this cluster of genes was strongly enriched for type I interferon signalling (data not shown). Moreover, prior knowledge based reconstruction of the wiring diagram of

the underlying gene networks for each cluster revealed that IRF7 – a master regulator of type I interferon responses,[32] was the dominant hub gene identified in cluster G5. Accordingly, we designated the children in clusters S1 and S2 as IRF7^{hi} versus IRF7^{lo} molecular phenotypes.

Network hubs and driver genes underlying IRF7^{hi} versus IRF7^{lo} molecular phenotypes

To further characterize the IRF7 phenotypes, children with exacerbations were stratified into IRF7^{hi} (n=26) and IRF7^{lo} (n=19) subgroups, and compared with RV negative controls employing LIMMA/SVA. We followed this strategy because a direct comparison of IRF7$^{hi/low}$ phenotypes would only reveal differences between the respective responses, and we wanted to know if the phenotypes operate through discrete and/or overlapping pathways. The data showed that 208 genes were upregulated and 157 genes were downregulated in children with IRF7^{hi} exacerbations compared with controls (Figure 3a, left panel; Table S5). IRF7^{lo} exacerbations were characterized by upregulation of 96 genes, and downregulation of 31 genes downregulated (Figure 3a, right panel; Table S6). These analyses revealed an overlapping response signature, which comprised 52 upregulated genes and 11 downregulated genes. Gene network analysis revealed that IRF7 gene networks were upregulated in the children with IRF7^{hi} exacerbations (Figure 3b, left panel). IRF7^{lo} exacerbations lacked an IRF7 signature, and instead were characterized by upregulation of Th2-associated pathways (e.g. IL-4R, FCER1G, ARG1) and downregulation of IFNg (Figure 3b, right panel). We also built a combined network to illustrate the unique and overlapping gene network patterns for each phenotype (Figure 4).

Next we employed upstream regulator analysis to identify molecular drivers of IRF7^{hi} and IRF7^{lo} exacerbation responses.[28, 33] The data showed that IRF7^{hi} exacerbations were putatively driven by upregulation of IFNL1, IRF7, and interferon alpha signalling (Figure 3c, left panel, Table S7). In contrast, IRF7^{lo} exacerbations were predicted to be driven by upregulation of cytokine and growth factor signalling pathways (e.g. IL-6, IL-10, TGFb, ERK, CSF3, EGF, Figure 3c, right panel, Table S8). It is noteworthy that multiple inflammatory pathways (e.g. IL-1b, IL-2, IL-4, IL-13, TNF, OSM, IFNG) featured in the upstream regulator analysis results for IRF7^{lo} exacerbations, however the activation Z-scores were not

significant, indicating that the direction of the gene expression changes in terms of up- and down- regulation were not consistent with the known role of these pathways in the regulation of gene expression.[28]

We re-examined the cellular composition data from Figure 1 in IRF7^{hi} and IRF7^{lo} exacerbation responses, and we found that both phenotypes were associated with decreased proportions of cDCs, and similar proportions of M1 macrophages (Figure S2). Stratification of IRF7 phenotypes by RV detection revealed further heterogeneity, including upregulated proportions of Th2 cells in children with RV positive, IRF7^{lo} exacerbations (Figure S3).

Candidate pathways linking exacerbation responses with asthma-related traits

To identify candidate pathways that potentially link exacerbation responses with expression of asthma-related traits, we employed Pubmatrix[34] to screen the literature for relevant studies (Table S9). We found that multiple genes which were upregulated in children with IRF7^{hi} exacerbations (e.g. CASP1, CD274, CXCL11, DDX58, Haptoglobin, IFIH1, IRF7, P2RX7, PHF11, Selectin L, SERPING1, STAT1, TLR4, TLR5, TNFAIP3, TNFAIP6, TNFSF13B) or IRF7^{lo} exacerbations (e.g. AGR3, C3AR1, EPCAM, IL4R, LDLR, NCR1, OCLN, SERPINB2, SERPINB3, THBS1, TIMP1, VCAN) have been previously studied in the context of asthma and/or related traits. Moreover, overlap signature of genes that were commonly upregulated in children with IRF7^{hi} and IRF7^{lo} exacerbations have also been previously studied in this context (e.g. ADAM17, ARG1, ARG2, CD163, CD38, FCER1G, IL18R1, PLA2G4A, S100A12, TLR2).

Clinical characteristics of IRF7^{hi} versus IRF7^{lo} exacerbations

We next investigated the biological and clinical characteristics of IRF7^{hi} and IRF7^{lo} exacerbations. These groups were not related to any technical variables measured in the study (Table S10). There was also no difference in season of recruitment, the detection of viral or bacterial pathogens, or the use of medications (Table 2). The prevalence of atopy, including allergy to aeroallergens, was higher in IRF7^{hi} exacerbations (76.9% and 73.1%, respectively) compared with IRF7^{lo} exacerbations (42.1% and 31.6%, p = 0.029 and 0.008,

respectively). Children with IRF7^{lo} exacerbations presented to hospital much later after initial symptoms (4.74 (SD 4.03) days) than IRF7^{hi} exacerbations (2.31 (SD 1.98) days, p = 0.011). This was also reflected in the duration of cough prior to hospitalization (IRF7^{lo}: 5.62 (SD 3.20) days and IRF7^{hi}: 1.96 (SD 1.51) days, respectively, p = 0.000027). Children with IRF7^{lo} exacerbations were at least 4.6 times more likely to be admitted to hospital compared with IRF7^{hi} exacerbations (OR 4.65, p = 0.018). Time to subsequent first representation/admission to hospital with an exacerbation was shorter in IRF7^{lo} exacerbations compared with IRF7^{hi} exacerbations (Table 2, Fig S5). Within the first year of follow-up, more children with IRF7^{lo} (68.4%) represented/readmitted to hospital with a respiratory exacerbation compared to those with IRF7^{hi} (30.8%, p = 0.017). All associations remained significant after adjustment for age, gender, aeroallergen allergy and Caucasian ethnicity.

Replication of IRF7^{hi} and IRF7^{low} exacerbation responses in an independent sample of children

To determine if IRF7^{hi} and IRF7^{lo} exacerbation phenotypes and their clinical correlates could be found in another group of children, RT-qPCR was employed to measure gene expression patterns in nasal swab samples from an independent sample of children. To select a panel of genes for RT-qPCR analysis, we focused on genes that were representative of IRF7^{hi} exacerbations (DDX60, IFNL1, IRF7, ISG15, Mx1, RSAD2, and the downregulated gene IL-33, Figure 4), IRF7^{lo} exacerbations (NCR1, THBS1, Figure 4), or that were common to both phenotypes (ARG1, CD163, FCER1G, IL-1R2, IL-18R1, TLR2, Figure 4). The RT-qPCR data was normalised to three endogenous control genes (HMBS, PPIA, PPIB), creating three separate variables for each gene, which were utilised for consensus clustering. The analysis segregated the subjects into five clusters (Figure 5); three of these had elevated expression of IRF7/interferon responses (combined as IRF7^{hi}; black dendrogram in Figure 5), and the remaining two clusters had low IRF7/interferon responses (IRF7^{low1} and IRF7^{low2}; red and green dendrograms respectively in Figure 5). A longer time lag was observed from first symptoms to hospital presentation in the IRF7^{low1} subjects (3.90 (SD 4.59) days) compared with the IRF7^{hi} group (2.20 (SD 1.76) days, p = 0.023). These symptoms included cough (p=0.015), wheeze (p=0.022) and shortness of breath (p = 0.02). Fever was more prevalent

in the IRF7^{hi} group (59.2%) compared with the IRF7^{low1} and IRF7^{low2} groups (24.1%, p = 0.004 and 10.0%, p < 0.001, respectively). Runny nose was also more prevalent in the IRF7^{hi} group (75.5%) compared to the IRF7^{low2} group (45.0%, p = 0.024). All associations remained significant after adjusting for age, gender, aeroallergy and Caucasian ethnicity.

Discussion

Our study is the first to investigate acute wheeze/asthma exacerbation phenotypes in children using a systems biology approach. We have confirmed the central role of IRF7 as a gene network hub and have identified two distinct IRF7 molecular phenotypes, IRF7^{hi} exhibiting robust upregulation of the Th1/type I interferon response and IRF7^{lo} with an alternative activation signature marked by upregulation of cytokine and growth factor signalling and downregulation of interferon gamma. Importantly, the two phenotypes also produced distinct clinical phenotypes. Compared with children with IRF7^{hi}, those with IRF7^{lo} had a slower progression of illness from initial symptoms to hospital presentation, a greater likelihood of a hospital admission, and a greater chance of representation with a further exacerbation. Exacerbation severity at presentation was not different between the two IRF7 patterns, perhaps because presentation to hospital is likely to be determined by symptoms reaching a severity threshold that causes parental concern. However also worth noting is that the apparently impaired IRF7 response in IRF7^{lo} children was not associated with an increase in exacerbation severity at presentation, although perhaps expectedly the reduced IRF7 response was associated with slower resolution of the episode. These findings were unaffected by the respiratory viruses or bacteria detected and medication use. Investigation of a replication cohort using RT-qPCR produced similar findings despite variations in the subject characteristics between the discovery and replication cohorts. In summary our findings reveal two distinct phenotypes with clear differences in gene regulation patterns, either upregulation of robust innate immune responses or cytokine and growth factor signalling, and associated differences in clinical characteristics.

Asthma and wheezing exacerbations are largely triggered by RV infections but the underlying mechanisms are not well understood.[2] Previous *in vitro* studies suggested that

RV-induced interferon responses were deficient in bronchial epithelial cells from subjects with asthma, resulting in increased viral loads and exaggerated secondary responses.[3, 4, 35] However, *in vivo* studies of immune response patterns in the airways of both children and adults with RV-induced exacerbations found that interferon responses were increased, not deficient.[9-11, 36] Moreover, a clinical trial that evaluated the utility of inhaled interferon beta therapy in adults at the first signs of a cold to prevent worsening of their asthma symptoms failed to achieve its primary endpoint.[37] Our data extend these previous findings by demonstrating that wheezing exacerbations in children are heterogeneous and characterised by two very different IRF7 molecular phenotypes. Upstream regulator analysis suggested that IRF7^{hi} exacerbations were driven by upregulation of IFNL1, IRF7, and interferon alpha signalling. In contrast, IRF7^{lo} exacerbations were putatively driven by upregulation of cytokine and growth factor signalling (i.e. IL-6, IL-10, TGFb, CSF3, EGF) and downregulation of interferon gamma.

IRF7 is a master regulator of type I and type III interferon gene expression.[32, 38-40] We previously reported that IRF7 gene networks were upregulated in nasal wash samples from asthmatic children experiencing mild-to-moderate viral exacerbations.[10] We have also shown that IRF7 promotes RV-induced innate antiviral responses and limits IL-33 mRNA expression in cultured bronchial epithelial cells,[33] and furthermore in our current study IL-33 was downregulated in IRF7^{hi} exacerbation responses. Girkin *et al*. reported that knockdown of IRF7 abolished RV-induced type I interferon responses in the airways in a mouse model.[40] Together, these experimental findings support our computational analysis unveiling IRF7 as a regulator of the gene networks underlying the IRF7^{hi} responder phenotype.

Children with IRF7^{lo} exacerbations in the discovery cohort exhibited a delayed progression from first symptom onset to hospital presentation. Given that our study design entailed recruitment of children at ED presentation, we could not determine if IRF7 gene networks were initially upregulated closer to the onset of infection and subsequently waned, or alternatively if they were never upregulated in the first place. To address this issue, an alternative study design would be required which entails regular sampling of exacerbation-prone children during the RV season.[41] It would also be of interest to further study the stability of these identified phenotypes to learn if subjects experience the same type of

response over multiple wheezing exacerbation events or not. Notwithstanding this, our replication cohort comprised approximately twice as many cases as the discovery cohort, and this larger sample enabled the identification and characterization of two subgroups of IRF7^{lo} children, and only one of these subgroups was characterized by delayed progression. The activation of growth factor signalling pathways and downregulation of interferon gamma may reflect the immune response entering a resolution phase, however, at the same time these children were symptomatic. Moreover, many were also RV positive, and given that TGFb signalling promotes rhinovirus replication, upregulation of this pathway may prolong infection and delay viral clearance.[42, 43] It is also known that frequent severe exacerbations are associated with deficits in lung function growth (children) and accelerated lung function decline (adults).[44] Thus repeated cycles of inflammation, growth factor signalling and repair may alter the structure and function of the airways underlying this phenotype.

The mechanisms that determine expression of disease symptoms amongst children with IRF7^{hi} and IRF7^{lo} exacerbations are unknown. Given that children with IRF7^{hi} exacerbations elicit robust antiviral responses, one possibility is that the airways of these children are sensitive to the host response to respiratory viruses. In this regard, several pathways associated with the IRF7^{hi} phenotype are known to impact on respiratory function. PD-L1 (encoded by CD274) is an immune checkpoint that delivers an inhibitory signal for T cell activation. Upregulation of PD-L1 during respiratory bacterial infections in early life suppresses the IL-13 decoy receptor IL-13Ra2, resulting in persistent airways hyperresponsiveness.[45] MDA5 (encoded by IFIH1) is a pattern recognition receptor that senses RV-derived RNA. MDA5 deficient mice infected with RV have delayed type I interferon responses, impaired type III interferon responses, and reduced airways hyperresponsiveness.[46] The proinflammatory effectors TNF, IFNg, and interferon gamma-induced protein 10 can also promote airway hyper-responsiveness in animal models.[47-49]

Another possibility is that IRF7^{hi} and IRF7^{lo} exacerbation responses converge on a final common pathway to precipitate respiratory symptoms (Figure 4). For example, CD38 is a receptor with enzymatic activity, which hydrolyses NAD, generating reaction products that modulate calcium signalling. It is expressed on immune and airway smooth muscle cells, and

it plays a dual role in asthma by enhancing airways inflammation and contractile responses in smooth muscle.[50] FCER1G is a component of the high affinity IgE receptor. Anti-IgE therapy neutralises serum IgE, reduces the expression of the high affinity IgE receptor on dendritic cells and mast cells, and it also reduces the frequency of asthma exacerbations.[51, 52] Phospholipases A2 are involved in the generation of eicosanoids from arachidonic acid. Knock-in of human sPLA2 into mice enhances airways inflammation and airways hyperresponsiveness.[53] TLR2 is a pattern recognition receptor that acts as a sensor for RV capsid.[54] In a mouse model of combined RV and allergen exposure, TLR2 signaling in macrophages was required for induction of airways inflammation and airways hyperresponsiveness.[55] In summary, our data has identified multiple candidate pathways that link IRF7^{hi} and IRF7^{lo} exacerbation responses with expression of respiratory symptoms, and these pathways represent logical candidates for future drug development programs.

This study has limitations that should be acknowledged. The expression profiles were derived from nasal swab samples that comprised a mixed cell population. Follow-up studies employing focused analyses in individually isolated cell types or single cell transcriptomics will be required to dissect the role of specific subpopulations of cells in this disease. The study participants were sampled during natural exacerbations, and it is not possible to control for all of the variables that may potentially impact on the data (e.g. age, gender, ethnicity, natural allergen exposure, pathogen strains and combinations, medications). To address this issue, our analysis strategy employed surrogate variable analysis to systematically estimate and adjust the analysis for all sources of hidden biological and/or technical variation. Some of the clinical characteristics associated with IRF7 phenotypes in the discovery cohort did not replicate in the validation cohort. This may be due in part to variations in the demographics and clinical characteristics between the two cohorts, as well as the fact that IRF7 phenotypes were defined in the discovery cohort by microarray analysis of a large number of genes, whereas in the validation cohort it was based on RT-qPCR analysis of a restricted gene panel. Finally, while our analyses have characterised gene network patterns underlying exacerbation phenotypes and unveiled candidate molecular drivers of the responses, further studies will be required to dissect the mechanisms that give rise to these phenotypes and drive the expression of respiratory symptoms. Notwithstanding these limitations, our findings demonstrate that exacerbation responses in

children are heterogeneous and comprise IRF7^{hi} versus IRF7^{lo} molecular phenotypes that determine clinical phenotypes. Future clinical trials targeting the interferon system in this disease should be stratified on the basis of these IRF7 phenotypes.

Author Contributions

Conception and design of the study: PNS, IAL, AB; Acquisition of data: SKK, KF, JB, NT, FP, JE, SO, MB; Data analysis and interpretation: SKK, JR, GZ, LC, CM, LO, NT, RM, PNS, IAL, AB; Drafting the manuscript for important intellectual content: SKK, PNS, IAL, AB; all authors reviewed and approved the final manuscript.

Acknowledgements

We thank all the children and their families who agreed to take part in the study. The study was funded by National Health and Medical Research Council (NHMRC APP1045760) and AstraZeneca. JB was funded by a Thoracic Society of Australia and New Zealand/AstraZeneca Respiratory Research Fellowship. LC is a recipient of the Asthma Foundation Fiona Staniforth and Australian Government Research Training Program Scholarships. NT is funded by the Mickey Hardy Asthma Australia National Scholarship. AB is supported by Fellowships from the Simon Lee Foundation and the Brightspark and McCusker Foundations.

References

1. Coleman L, Laing IA, Bosco A. Rhinovirus-induced asthma exacerbations and risk populations. Curr Opin Allergy Clin Immunol 2016.
2. Bizzintino J, Lee WM, Laing IA, Vang F, Pappas T, Zhang G, et al. Association between human rhinovirus C and severity of acute asthma in children. Eur Respir J 2011; 37:1037-42.
3. Wark PA, Johnston SL, Bucchieri F, Powell R, Puddicombe S, Laza-Stanca V, et al. Asthmatic bronchial epithelial cells have a deficient innate immune response to infection with rhinovirus. The Journal of experimental medicine 2005; 201:937-47.
4. Contoli M, Message SD, Laza-Stanca V, Edwards MR, Wark PA, Bartlett NW, et al. Role of deficient type III interferon-lambda production in asthma exacerbations. Nature medicine 2006; 12:1023-6.
5. Ritchie AI, Farne HA, Singanayagam A, Jackson DJ, Mallia P, Johnston SL. Pathogenesis of Viral Infection in Exacerbations of Airway Disease. Ann Am Thorac Soc 2015; 12 Suppl 2:S115-32.
6. Beale J, Jayaraman A, Jackson DJ, Macintyre JD, Edwards MR, Walton RP, et al. Rhinovirus-induced IL-25 in asthma exacerbation drives type 2 immunity and allergic pulmonary inflammation. Sci Transl Med 2014; 6:256ra134.
7. Jackson DJ, Makrinioti H, Rana BM, Shamji BW, Trujillo-Torralbo MB, Footitt J, et al. IL-33-Dependent Type 2 Inflammation during Rhinovirus-induced Asthma Exacerbations In Vivo. Am J Respir Crit Care Med 2014; 190:1373-82.

8. Murray CS, Poletti G, Kebadze T, Morris J, Woodcock A, Johnston SL, et al. Study of modifiable risk factors for asthma exacerbations: virus infection and allergen exposure increase the risk of asthma hospital admissions in children. Thorax 2006; 61:376-82.
9. Bosco A, Ehteshami S, Stern DA, Martinez FD. Decreased activation of inflammatory networks during acute asthma exacerbations is associated with chronic airflow obstruction. Mucosal immunology 2010; 3:399-409.
10. Bosco A, Ehteshami S, Panyala S, Martinez FD. Interferon regulatory factor 7 is a major hub connecting interferon-mediated responses in virus-induced asthma exacerbations in vivo. The Journal of allergy and clinical immunology 2012; 129:88-94.
11. Miller EK, Hernandez JZ, Wimmenauer V, Shepherd BE, Hijano D, Libster R, et al. A mechanistic role for type III IFN-lambda1 in asthma exacerbations mediated by human rhinoviruses. American journal of respiratory and critical care medicine 2012; 185:508-16.
12. Qureshi F, Pestian J, Davis P, Zaritsky A. Effect of nebulized ipratropium on the hospitalization rates of children with asthma. N Engl J Med. 1998; 339:1030-5.
13. Bentur L, Canny GJ, Shields MD, Kerem E, Schuh S, Reisman JJ, et al. Controlled trial of nebulized albuterol in children younger than 2 years of age with acute asthma. Pediatrics 1992; 89:133-7.
14. Chidlow GR, Harnett GB, Shellam GR, Smith DW. An economical tandem multiplex real-time PCR technique for the detection of a comprehensive range of respiratory pathogens. Viruses 2009; 1:42-56.
15. Lee WM, Lemanske RF, Jr., Evans MD, Vang F, Pappas T, Gangnon R, et al. Human rhinovirus species and season of infection determine illness severity. Am J Respir Crit Care Med 2012; 186:886-91.
16. Bochkov YA, Grindle K, Vang F, Evans MD, Gern JE. Improved molecular typing assay for rhinovirus species A, B, and C. J Clin Microbiol 2014; 52:2461-71.
17. Irizarry RA, Hobbs B, Collin F, Beazer-Barclay YD, Antonellis KJ, Scherf U, et al. Exploration, normalization, and summaries of high density oligonucleotide array probe level data. Biostatistics 2003; 4:249-64.
18. Dai M, Wang P, Boyd AD, Kostov G, Athey B, Jones EG, et al. Evolving gene/transcript definitions significantly alter the interpretation of GeneChip data. Nucleic acids research 2005; 33:e175.
19. Kauffmann A, Gentleman R, Huber W. arrayQualityMetrics--a bioconductor package for quality assessment of microarray data. Bioinformatics 2009; 25:415-6.
20. McCall MN, Murakami PN, Lukk M, Huber W, Irizarry RA. Assessing affymetrix GeneChip microarray quality. BMC bioinformatics 2011; 12:137.
21. Smyth GK. limma: Linear Models for Microarray Data. In: Gentleman R, Carey VJ, Huber W, Irizarry RA, Dudoit S, editors. Bioinformatics and Computational Biology Solutions Using R and Bioconductor. New York, NY: Springer New York; 2005. p. 397-420.
22. Leek JT, Storey JD. Capturing heterogeneity in gene expression studies by surrogate variable analysis. PLoS Genet 2007; 3:1724-35.
23. Lu J, Kerns RT, Peddada SD, Bushel PR. Principal component analysis-based filtering improves detection for Affymetrix gene expression arrays. Nucleic Acids Res 2011; 39:e86.

24. Wilkerson MD, Hayes DN. ConsensusClusterPlus: a class discovery tool with confidence assessments and item tracking. Bioinformatics 2010; 26:1572-3.
25. Jacob L, Gagnon-Bartsch JA, Speed TP. Correcting gene expression data when neither the unwanted variation nor the factor of interest are observed. Biostatistics 2016; 17:16-28.
26. Freytag S, Gagnon-Bartsch J, Speed TP, Bahlo M. Systematic noise degrades gene co-expression signals but can be corrected. BMC Bioinformatics 2015; 16:309.
27. Chen EY, Tan CM, Kou Y, Duan Q, Wang Z, Meirelles GV, et al. Enrichr: interactive and collaborative HTML5 gene list enrichment analysis tool. BMC Bioinformatics 2013; 14:128.
28. Kramer A, Green J, Pollard J, Jr., Tugendreich S. Causal analysis approaches in Ingenuity Pathway Analysis. Bioinformatics 2014; 30:523-30.
29. Aran D, Hu Z, Butte AJ. xCell: Digitally portraying the tissue cellular heterogeneity landscape. bioRxiv 2017.
30. Spandidos A, Wang X, Wang H, Seed B. PrimerBank: a resource of human and mouse PCR primer pairs for gene expression detection and quantification. Nucleic Acids Res 2010; 38:D792-9.
31. Newman AM, Liu CL, Green MR, Gentles AJ, Feng W, Xu Y, et al. Robust enumeration of cell subsets from tissue expression profiles. Nat Methods 2015; 12:453-7.
32. Honda K, Yanai H, Negishi H, Asagiri M, Sato M, Mizutani T, et al. IRF-7 is the master regulator of type-I interferon-dependent immune responses. Nature 2005; 434:772-7.
33. Bosco A, Wiehler S, Proud D. Interferon regulatory factor 7 regulates airway epithelial cell responses to human rhinovirus infection. BMC Genomics 2016; 17:76.
34. Becker KG, Hosack DA, Dennis G, Jr., Lempicki RA, Bright TJ, Cheadle C, et al. PubMatrix: a tool for multiplex literature mining. BMC Bioinformatics 2003; 4:61.
35. Baraldo S, Contoli M, Bazzan E, Turato G, Padovani A, Marku B, et al. Deficient antiviral immune responses in childhood: Distinct roles of atopy and asthma. The Journal of allergy and clinical immunology 2012; 130:1307-14.
36. Hansel TT, Tunstall T, Trujillo-Torralbo MB, Shamji B, Del-Rosario A, Dhariwal J, et al. A Comprehensive Evaluation of Nasal and Bronchial Cytokines and Chemokines Following Experimental Rhinovirus Infection in Allergic Asthma: Increased Interferons (IFN-gamma and IFN-lambda) and Type 2 Inflammation (IL-5 and IL-13). EBioMedicine 2017; 19:128-38.
37. Djukanovic R, Harrison T, Johnston SL, Gabbay F, Wark P, Thomson NC, et al. The effect of inhaled IFN-beta on worsening of asthma symptoms caused by viral infections. A randomized trial. Am J Respir Crit Care Med 2014; 190:145-54.
38. Osterlund PI, Pietila TE, Veckman V, Kotenko SV, Julkunen I. IFN regulatory factor family members differentially regulate the expression of type III IFN (IFN-lambda) genes. Journal of immunology 2007; 179:3434-42.
39. Ciancanelli MJ, Huang SX, Luthra P, Garner H, Itan Y, Volpi S, et al. Infectious disease. Life-threatening influenza and impaired interferon amplification in human IRF7 deficiency. Science 2015; 348:448-53.
40. Girkin J, Hatchwell L, Foster P, Johnston SL, Bartlett N, Collison A, et al. CCL7 and IRF-7 Mediate Hallmark Inflammatory and IFN Responses following Rhinovirus 1B Infection. J Immunol 2015; 194:4924-30.

41. Olenec JP, Kim WK, Lee WM, Vang F, Pappas TE, Salazar LE, et al. Weekly monitoring of children with asthma for infections and illness during common cold seasons. The Journal of allergy and clinical immunology 2010; 125:1001-6 e1.
42. Baines KJ, Simpson JL, Wood LG, Scott RJ, Gibson PG. Transcriptional phenotypes of asthma defined by gene expression profiling of induced sputum samples. The Journal of allergy and clinical immunology 2011; 127:153-60, 60 e1-9.
43. Bedke N, Sammut D, Green B, Kehagia V, Dennison P, Jenkins G, et al. Transforming growth factor-beta promotes rhinovirus replication in bronchial epithelial cells by suppressing the innate immune response. PLoS One 2012; 7:e44580.
44. Dougherty RH, Fahy JV. Acute exacerbations of asthma: epidemiology, biology and the exacerbation-prone phenotype. Clinical and experimental allergy : journal of the British Society for Allergy and Clinical Immunology 2009; 39:193-202.
45. Starkey MR, Nguyen DH, Brown AC, Essilfie AT, Kim RY, Yagita H, et al. Programmed Death Ligand 1 Promotes Early-Life Chlamydia Respiratory Infection-Induced Severe Allergic Airway Disease. Am J Respir Cell Mol Biol 2016; 54:493-503.
46. Wang Q, Miller DJ, Bowman ER, Nagarkar DR, Schneider D, Zhao Y, et al. MDA5 and TLR3 initiate pro-inflammatory signaling pathways leading to rhinovirus-induced airways inflammation and hyperresponsiveness. PLoS pathogens 2011; 7:e1002070.
47. Choi IW, Sun K, Kim YS, Ko HM, Im SY, Kim JH, et al. TNF-alpha induces the late-phase airway hyperresponsiveness and airway inflammation through cytosolic phospholipase A(2) activation. J Allergy Clin Immunol 2005; 116:537-43.
48. Kanda A, Driss V, Hornez N, Abdallah M, Roumier T, Abboud G, et al. Eosinophil-derived IFN-gamma induces airway hyperresponsiveness and lung inflammation in the absence of lymphocytes. J Allergy Clin Immunol 2009; 124:573-82, 82 e1-9.
49. Medoff BD, Sauty A, Tager AM, Maclean JA, Smith RN, Mathew A, et al. IFN-gamma-inducible protein 10 (CXCL10) contributes to airway hyperreactivity and airway inflammation in a mouse model of asthma. J Immunol 2002; 168:5278-86.
50. Gally F, Hartney JM, Janssen WJ, Perraud AL. CD38 plays a dual role in allergen-induced airway hyperresponsiveness. Am J Respir Cell Mol Biol 2009; 40:433-42.
51. Prussin C, Griffith DT, Boesel KM, Lin H, Foster B, Casale TB. Omalizumab treatment downregulates dendritic cell FcepsilonRI expression. J Allergy Clin Immunol 2003; 112:1147-54.
52. Busse WW, Morgan WJ, Gergen PJ, Mitchell HE, Gern JE, Liu AH, et al. Randomized trial of omalizumab (anti-IgE) for asthma in inner-city children. The New England journal of medicine 2011; 364:1005-15.
53. Henderson WR, Jr., Oslund RC, Bollinger JG, Ye X, Tien YT, Xue J, et al. Blockade of human group X secreted phospholipase A2 (GX-sPLA2)-induced airway inflammation and hyperresponsiveness in a mouse asthma model by a selective GX-sPLA2 inhibitor. J Biol Chem 2011; 286:28049-55.
54. Triantafilou K, Vakakis E, Richer EA, Evans GL, Villiers JP, Triantafilou M. Human rhinovirus recognition in non-immune cells is mediated by Toll-like receptors and MDA-5, which trigger a synergetic pro-inflammatory immune response. Virulence 2011; 2:22-9.
55. Han M, Chung Y, Young Hong J, Rajput C, Lei J, Hinde JL, et al. Toll-like receptor 2-expressing macrophages are required and sufficient for rhinovirus-induced airway inflammation. J Allergy Clin Immunol 2016; 138:1619-30.

597 **Figure Titles and Legends**

598

599 **Figure 1. Computational inference of the cellular composition of the nasal swab samples.**
600 **A)** Relative proportions of 12 major cell types across the cohort. **B)** Relative proportions of
601 individual cell types stratified according to RV status (RV+, RV-) within wheeze (Whz),
602 convalescent (Conv) and control (Ctrl) subjects. **C)** Relationship between cell type
603 proportions and clinical traits. Proportions were determined by computational
604 deconvolution. Boxplots show IQR fenced using the Turkey method. Significant two-way
605 Kruskal-Wallis P values are shown in italics. * represents a Mann-Whitney P value < 0.05, **
606 < 0.01, *** < 0.001, and **** < 0.0001.

607

608 **Figure 2. Discovery of IRF7 molecular phenotypes. A)** Consensus hierarchical clustering was
609 performed on gene expression profiles derived from nasal swab samples. Five clusters of
610 subjects (S1-S5) and genes (G1-G5) were identified. **B)** The expression profiles of each gene
611 cluster were summarized by principal components analysis, and the first principal
612 component of each gene cluster was plotted across the subjects stratified by their cluster
613 membership. **C)** Experimentally supported findings from published studies (prior
614 knowledge) were employed to reconstruct the wiring diagram of the gene networks for
615 each gene cluster. Genes colored red were upregulated and those colored green were
616 downregulated in subjects from cluster S1 versus S2. Solid/dashed lines indicate
617 direct/indirect functional relationships between genes. Larger nodes have more
618 connections.

619

620 **Figure 3. Identification of network hubs and driver genes underlying IRF7hi and IRF7lo**
621 **exacerbations. A)** Differentially expressed genes were identified by comparing children with
622 IRF7hi exacerbations (left panel) or IRF7lo exacerbations (right panel) with RV negative
623 controls. Data are presented as volcano plots, and the dashed horizontal line represents FDR
624 = 0.05. **B)** The gene networks underlying IRF7hi exacerbations (left panel) or IRF7lo
625 exacerbations (right panel) were reconstructed employing prior knowledge. Genes colored
626 red were upregulated and genes colored green were downregulated. Larger nodes have
627 more connections. **C)** Upstream regulator analysis was employed to infer molecular drivers
628 of IRF7hi (left panel) and IRF7lo (right panel) exacerbations. The drivers were ranked by –

Log10 overlap p-value or activation Z-score. Red bars indicate pathway activation (activation Z-score greater than 2.0) and blue bars indicate pathway inhibition (activation Z-score less than -2.0). White bars indicate pathways with non-significant activation Z-scores (i.e. absolute Z-scores less than 2.0).

Figure 4: IRF7hi and IRF7lo exacerbation phenotypes operate through discrete and overlapping pathways. Gene networks associated with IRF7hi exacerbations (left side), IRF7lo exacerbations (right side), or common to both responses (middle). Genes are organised by subcellular location. Genes colored red were upregulated and those colored green were downregulated relative to RV negative controls.

Figure 5. Identification of IRF7hi and IRF7lo exacerbations phenotypes in an independent cohort of children. Gene expression patterns were profiled by RT-qPCR in nasal swab samples collected from children with an asthma/wheezing exacerbation (red columns) or healthy controls (black columns). The RT-qPCR data was normalised separately to three independent endogenous reference genes, resulting in three variables for each target gene, and then analysed by consensus hierarchical cluster analysis. The dendrogram is colored by phenotype (IRF7hi = black, IRF7low1 green, IRF7low1 red).

Figure Titles

Table 1. Characteristics of the study population.

Table 2. Characteristics of the IRF7hi and IRF7lo phenotypes in the discovery and replication cohorts.

Method

Study Participants

The participants were part of an ongoing study examining the mechanisms of acute viral respiratory infection in children (MAVRIC). Cases were children aged 0-16 years presenting

to the ED of a tertiary children's hospital (Princess Margaret Hospital, Perth, Western Australia) with acute wheeze and the availability of nasal fluid and swab specimens. All respiratory diagnoses were determined by the treating physician and were independent of study staff. Controls consisted of siblings of the cases or randomly selected children from the community. We defined 'admission to hospital' as admission to a non-ED hospital ward. We also collected 19 convalescent/quiescent nasal samples from children who were followed-up at least 6 weeks after an acute exacerbation of asthma or wheeze; only a subset of these samples (5/19) were paired with acute samples. The hospital's Human Ethics Committee approved the study (MAVRIC approval 1761 EP) and parental/guardian written informed consent was obtained prior to recruitment. An independent sample of children from within the MAVRIC cohort was used as a validation cohort.

Data and sample collection

A detailed questionnaire and medical records were used to provide demographic and medical information for each participant during recruitment and follow-up. A child was considered positive for aeroallergy if they had a positive response to either (1) the skin prick test completed on 9 allergens (rye grass, mixed grasses, dog, cat, cockroach, *Alternaria tenuis*, *Aspergillus fumigatus*, *Dermatophagoides farinae*, *D. pteronyssinus*), or (2) a positive specific IgE to either cat or house dust mite (>0.35kU/L) at either the acute or convalescent visit, or positive answers to the acute questionnaire for the questions "Does your child suffer from hayfever?", or "Does your child suffer from allergies to: (a) grasses/pollens?; or (b) dust mite?". A child was considered positive for allergy overall if they had (1) aeroallergy; or (2) a positive response to the skin prick tests for either cows' milk or egg white, or (3) a parental report of a history of anaphylaxis, or (4) a high total IgE at either the acute or convalescent visit.

Acute asthma severity scores were assigned to each child at recruitment using a modified National Institute of Health score for children over 2 years of age[12] and included assessments of respiratory rate appropriate for age, oxygen saturation, auscultation, retractions and dyspnea. A separate, age-appropriate severity score was used for children aged under 2 years[13] with assessments of heart rate, respiratory rate, wheezing and

692 accessory muscle use. Separate severity Z scores were calculated for each child within each
693 of the two age groups to provide standardized scores across the whole cohort.
694
695 The time to next re-presentation or admission to a public hospital in Western Australian
696 with any acute respiratory illness for each child, within the first and second year of
697 observation, was obtained from the state hospital database retrospectively.
698
699 A nasal secretion sample from each participant was collected to test for the presence of
700 respiratory viruses and bacteria. Nasal swab specimens were obtained from each child using
701 flocked swabs (Copan, Italy) and were taken immediately to the laboratory for processing
702 for gene expression profiling.
703
704 *Virus and bacteria detection*
705 Common respiratory pathogens (adenovirus, respiratory syncytial virus (RSV) types A and B,
706 bocavirus, coronavirus, parainfluenza viruses 1-4, influenza viruses A, B and C,
707 metapneumovirus, *Bordetella* species, *Mycoplasma pneumoniae*, *Chlamydophila*
708 *pneumoniae*, *Haemophilus influenzae*, *Pneumocystis jirovecii*, *Staphylococcus aureus*,
709 *Streptococcus Pneumoniae* and *pyogenes*) were identified using a tandem multiplex real-
710 time PCR assay as previously described.[14] Rhinovirus (RV) was detected and genotyped by a
711 molecular method as previously described.[15, 16]
712
713 *Microarray analysis of gene expression*
714 Total RNA was extracted from nasal swabs using TRIzol (Invitrogen) followed by RNeasy
715 MinElute (QIAgen).[10] The quality and integrity of the RNA was analysed on the nanodrop
716 and bioanalyzer (Agilent). Total RNA samples were shipped on dry ice to the Ramaciotti
717 Centre for Genomics, at the University of New South Wales, Sydney, for processing and
718 hybridization to Human Gene 2.1 ST microarrays (Affymetrix). The raw microarray data are
719 available from the gene expression omnibus repository (accession: GSE103166).
720
721 *Microarray data analysis*
722 The microarray data was preprocessed in R employing the Robust Multi-Array (RMA)
723 algorithm.[17] A custom chip description file (hugene21sthsentrezg; version 20) was utilized to

map probe sets to genes.[18] The quality of the microarray data was assessed employing the R package arrayQualityMetrics. Low quality/outlying arrays were identified on the basis of Relative Log Expression (RLE) and Normalized Unscaled Standard Error (NUSE) metrics and removed from the analysis.[19, 20] Differentially expressed genes were identified using Linear Models for Microarray Data (LIMMA) in conjunction with Surrogate Variable Analysis (SVA).[21, 22] Limma entails fitting a linear model to the log expression intensities for each gene, and Empirical Bayes methods are employed to moderate the standard error estimates resulting in improved power and more stable inference.[21] Surrogate Variable Analysis estimates and captures all sources of hidden biological and/or technical variation that may potentially confound the analysis, and the estimated surrogate variables are added as covariates to the limma models. Where applicable, the correlation between paired samples was accounted for in the linear model fit through use of the duplicateCorrelation function. P-values derived from the limma models were adjusted for multiple testing employing the false discovery rate method.[21] Non-informative probe sets were identified using the proportion of variation accounted by the first principal component (PVAC) algorithm and filtered out of the results from the differential expression analysis.[23]

Discovery of molecular phenotypes

Molecular phenotypes were identified using consensus hierarchical clustering.[24] This algorithm employs data resampling techniques to find consensus across thousands of runs of a cluster analysis.[24] Prior to cluster analysis, batch-like effects and other sources of unwanted variation were modelled and removed using the RUVnormalize algorithm.[25] This algorithm leverages a set of negative control genes that are not associated with the outcome of interest to model unwanted variation and regress it out of the data. To select negative control genes, genes associated with wheezing exacerbations were first identified in case/control comparisons between wheezing/convalescent or wheezing/control samples using LIMMA/SVA, and those genes with an adjusted p-value less than 0.2 for any comparison were excluded from control gene selection. Negative control genes (n=1000) were selected from the remaining genes using the empNegativeControls function from the RUVCorr package.[26] After removal of unwanted variation using the RUVnormalize algorithm, the gene expression data was converted to Z-scores, and consensus hierarchical clustering was performed using the set of genes that were associated with the outcome of interest

(adjusted p-value < 0.1). Hierarchical cluster analysis was performed using Pearson correlation and ward linkage.

Pathways analysis

Pathways analysis was performed using Enrichr software and the Reactome database.[27]

Prior knowledge based reconstruction of gene networks

Gene networks were constructed employing experimentally supported findings from published studies curated in the Ingenuity Systems Knowledge Base (Ingenuity Systems, Redwood City, California). Direct and indirect molecular relationships were considered from all available categories, including activation, inhibition, localisation, modification, molecular cleavage, phosphorylation, protein-DNA interaction, protein-protein interaction, regulation of binding, transcription, translation, and ubiquitination. The circular layout was employed to display the network graph object, and hubs were positioned at the centre of the network. The nodes were coloured based on the expression ratio; red nodes denote upregulated genes and green nodes denote downregulation.

Upstream regulator analysis

Upstream regulator analysis (Ingenuity Systems, Redwood City, California) was employed to infer the molecular drivers of the observed differential gene expression patterns.[28] Two statistical metrics were calculated. The overlap p-value measures enrichment of known downstream target genes for a given upstream regulator amongst the differentially expressed genes. The activation Z-score is a measure of the pattern match between the direction of the observed gene expression changes (in terms of up/down regulation) and the predicted pattern based on prior experimental evidence. Pathways with an activation Z-score greater than 2.0 are predicted to be activated, and an activation Z-score less than -2.0 indicates pathway inhibition. If the activation Z-score lies between -2.0 and 2.0, the activation state of the pathway cannot be predicted.

Estimation of cellular composition from gene expression profiles

Cell type enrichment was examined in microarray-based gene expression profiles using the xCell webtool (University of California, San Francisco).[29] Gene signatures for 64 cell types

were determined from >1,800 transcriptomic profiles of purified cell samples allowing reliable enrichment analysis to investigate tissue heterogeneity. Cell types were chosen for further analysis based on their potential importance in the upper airways. Enrichment scores were converted to proportional cellular composition, allowed for by the linearity assumption, so that the sum of the proportions was equal to 1. Statistical comparisons were performed using nonparametric Kruskal-Wallis and Mann-Whitney U tests (GraphPad software [La Jolla, USA]).

RT-qPCR

Total RNA extracted from nasal swab samples was reverse-transcribed into cDNA using the QuantiTect Reverse Transcription Kit (Qiagen). qPCR was performed using QuantiFast SYBR Green PCR Master Mix (Qiagen) on the ABI 7900HT Sequence Detection System (Life Technologies). Primer sequences were obtained from Primerbank[30] and purchased from Sigma. Standard curves were prepared from serially diluted RT-qPCR products. Melt-curve analysis was conducted for all samples to confirm the specificity of amplified products. Relative expression levels of target genes were calculated by normalization to the housekeeping genes *HMBS*, *PPIA* and *PPIB*.[9] The RT-qPCR was log2 transformed, converted to Z-scores, and analyzed by consensus hierarchical clustering.

Statistical Analysis

Comparisons of all categorical variables between the clusters were performed using χ^2 test while ANOVA was used for continuous variables. Kaplan-Meier survival curve was used to assess the time to first re-presentation or admission after recruitment. A p-value of less than 0.05 was considered significant. All analyses were performed using SPSS version 22 (Chicago, Illinois).

Supplemental Information Titles and Legends

Figure S1: Identification of IRF7 molecular phenotypes by consensus clustering. A) The empNegativeControls function from the R package RUVCorr was employed to identify a set of negative controls genes. The plot shows variability on the vertical axis (IQR) versus mean expression on the horizontal axis. The control genes are coloured red. **B)** The RUVnormalise algorithm was employed to model unwanted variation and regress it out of the data. The

pairwise correlation between samples was calculated before (left panel) and after (right panel) RUV normalisation. Variations in cellular composition resulted in strong correlation patterns between samples, and this correlation structure was removed by RUV normalisation. **C)** The consensus clustering algorithm calculates a metric called the Cumulative Distribution Function (CDF), which measures consensus across hundreds of different clustering runs for increasing numbers of "k" clusters. The number of clusters in the data is estimated by observing the point at which the CDF reaches a maximum (left plot), and/or as the relative change in area under the CDF curve stabilises (right panel). In this data set, the CDF did not reach a maximum value, but the rate of change of the area under the curve started to plateau at k=5 or k=6. **D)** The consensus cluster analysis result was plotted for k=5 (left panel) and k=6 (right panel). We selected k=5 because the clusters were more well defined.

Figure S2: Computational inference of the cellular responses underlying IRF7hi and IRF7lo exacerbations. Relative proportions of 13 major cell types in nasal swab samples collected from children with IRF7hi exacerbations, IRF7lo exacerbations, or from healthy controls. Boxplots showing IQR fenced using the Turkey method. Significant two-way Kruskal-Wallis P values are shown in italics. * represents a Mann-Whitney P value < 0.05, ** < 0.01, *** < 0.001, and **** < 0.0001.

Figure S3: Computational inference of the cellular responses underlying IRF7hi and IRF7lo exacerbations stratified by RV detection. Relative proportions of 13 major cell types in nasal swab samples collected from children with IRF7hi exacerbations, IRF7lo exacerbations, or from healthy controls. Boxplots showing IQR fenced using the Turkey method. Significant two-way Kruskal-Wallis P values are shown in italics. * represents a Mann-Whitney P value < 0.05, ** < 0.01, *** < 0.001, and **** < 0.0001.

Figure S4: Time to next hospital presentation or admission for a respiratory illness comparing children in the discovery cohort with IRF7hi or IRF7lo exacerbations. Kaplan Meier curve of the proportion of children that have a subsequent hospital presentation/admission for any respiratory diagnosis followed for a maximum of 3.55 years.

851 Censored data represents the length of time a child was followed and did not have another
852 hospital presentation/admission for a respiratory illness.
853
854 **Table S1:** Differential gene expression in children with RV positive exacerbations vs RV
855 negative controls.
856 **Table S2:** Differential gene expression in children with RV positive exacerbations vs RV
857 negative convalescence.
858 **Table S3:** Differential gene expression in children with RV negative exacerbations vs RV
859 negative controls.
860 **Table S4:** Differential gene expression in children with RV negative exacerbations vs RV
861 negative convalescence.
862 **Table S5:** Differential gene expression in children with IRF7hi exacerbations vs RV negative
863 controls.
864 **Table S6:** Differential gene expression in children with IRF7lo exacerbations vs RV negative
865 controls.
866 **Table S7:** Molecular drivers of IRF7hi exacerbations.
867 **Table S8:** Molecular drivers of IRF7lo exacerbations.
868 **Table S9:** Pubmatrix results.
869 **Table S10:** Technical variables of samples in the IRF7hi and IRF7lo exacerbations.
870

Table 1: Characteristics of the study population.

	Discovery Cohort				Replication Cohort			
	Wheezing Exacerbation	Convalescence	Controls	Overall	Wheezing Exacerbation	Discov vs Replic	Controls	WE vs Ctrl
N	56	19	31	p-value	99	p-value	12	p-value
Age, mean (SD), yrs	4.35 (3.31)*	4.48 (1.62)	6.40 (4.41)	**0.027**	5.47 (3.61)	0.057	3.47 (3.16)	0.07
Male Gender, n/N (%)	30/56 (53.6)	12/19 (63.2)	15/31 (48.4)	0.63	62/99 (62.6)	0.309	4/12 (33.3)	0.053
Caucasian, n/N (%)	26/56 (46.4)*	13/19 (68.4)	22/28 (78.6)	**0.012**	47/96 (49.0)	0.867	8/8 (100)	**0.006**
Spring recruitment, n/N (%)	6/56 (10.7)#	8/19 (42.1)	8/31 (25.8)	**0.01**	27/99 (27.3)	**0.015**	1/12 (8.3)	0.289
Autumn recruitment, n/N (%)	6/56 (10.7)	4/19 (21.1)	6/31 (19.4)	0.383	28/99 (28.3)	**0.015**	5/12 (41.7)	0.336
Winter recruitment, n/N (%)	44/56 (78.6)*#	7/19 (36.8)	17/31 (54.8)	**0.002**	42/99 (42.4)	**<0.001**	6/12 (50.0)	0.76
Overall Allergy, n/N (%)	34/56 (60.7%)	7/11 (63.6)	18/28 (64.3%)	0.952	78/99 (78.8)	**0.024**	4/12 (33.3)	**0.002**
AeroAllergy, n/N (%)	31/56 (55.4)	7/11 (63.6)	16/28 (57.1)	0.954	70/99 (70.7)	0.079	3/12 (25.0)	**0.003**
Pathogen Detection								
Respiratory virus+, n/N (%)	47/54 (87.0)*##	8/19 (42.1)	18/31 (58.1)	**<0.001**	72/93 (77.4)	0.195	5/11 (45.5)	0.032
RV+, n/N (%)	37/56 (66.1)*#	5/19 (26.3)	10/31 (32.3)	**0.001**	64/97 (66.0)	1	5/11 (45.5)	0.199
RVC+, n/N (%)	26/56 (46.4)*	5/19 (26.3)	4/31 (12.9)	**0.004**	41/93 (44.1)	0.865	3/11 (27.3)	0.348
RVA+, n/N (%)	11/56 (19.6)	0/19 (0)	6/31 (19.4)	0.082	16/93 (17.2)	0.827	0/11 (0)	0.207
RSV+, n/N (%)	7/51 (13.7)	0/19 (0)	3/31 (9.7)	0.247	7/84 (8.3)	0.386	0/9 (0)	1
No. of viruses+, mean (SD)	1.13 (0.76)#, n=45	0.47 (0.61), n=19	0.87 (0.92), n=31	**0.011**	0.85 (0.64), n=81	**0.028**	0.56 (0.73), n=9	0.193
Bacteria+, n/N (%)	32/45 (71.1)	15/19 (78.9)	19/31 (61.3)	0.415	40/75 (53.3)	0.058	3/9 (33.3)	0.485

No. of bacteria +, mean (SD)	1.09 (0.90), n=45	1.21 (0.92), n=19	1.00 (1.00), n=31	0.743	0.71 (0.78), n=82	**0.014**	0.33 (0.50), n=9	0.163
No. of viruses+ and bacteria+, mean (SD)	2.22 (1.28), n=45	1.68 (0.95), n=19	1.87 (1.26), n=31	0.213	1.56 (1.08), n=81	**0.002**	0.89 (1.17), n=9	0.086
Symptoms								
Symptoms of URTI, n/N (%)	51/56 (91.1)				82/98 (83.7)	0.231		
Time from first symptom to recruitment, mean (SD), days	4.43 (3.61), n=56				3.48 (3.11), n=98	0.088		
Time from first symptom to hospital presentation, mean (SD), days	3.46 (3.33), n=56				2.62 (2.98), n=99	0.105		
Time from presentation to recruitment, mean (SD), days	20.44 (17.43), n=44				16.88 (11.89), n=77	0.186		
Current doctor-diagnosed wheeze, n/N (%)	56/56 (100)				99/99 (100)			
Severity z-score, mean (SD)	0.48 (0.81), n=53				0.57 (0.78), n=87	0.503		
Cough, n/N (%)	49/54 (90.7)				91/97 (93.8)	0.524		
Wheeze, n/N (%)	53/56 (94.6)				95/98 (96.9)	0.669		
Short of breath, n/N (%)	53/56 (94.6)				92/98 (93.9)	1		
Fever, n/N (%)	25/56 (44.6)				38/98 (38.8)	0.5		
Weak and tired, n/N (%)	29/56 (51.8)				55/98 (56.1)	0.618		
Runny nose, n/N (%)	40/56 (71.4)				65/98 (66.3)	0.591		
Congestion, n/N (%)	26/55 (47.3)				36/98 (36.7)	0.232		
Sneeze, n/N (%)	27/55 (49.1)				48/98 (49.0)	1		

Sore throat, n/N (%)	2/56 (3.6)	2/99 (2.0)	0.62
Hospital Admission and Medication			
Admitted to hospital, n/N (%)	27/56 (48.2)	42/99 (42.4)	0.505
Time to discharge, mean (SD), hrs	33.78 (22.39), n=54	33.83 (35.37), n=98	0.993
Steroid, n/N (%)	34/39 (87.2)	68/90 (75.6)	0.163
Time from steroid to sample collection, mean (SD), hrs	10.49 (11.71), n=32	8.73 (9.81), n=55	0.456
Antibiotics, n/N (%)	8/45 (17.8)	19/90 (21.1)	0.82

* $P < 0.05$ Wheezing Exacerbation compared to Controls

# $P < 0.05$ Wheezing Exacerbation compared to Convalescence

$P < 0.001$ Wheezing Exacerbation compared to Convalescence

Table 2: Characteristics of the IRF7^{hi} and IRF7^{lo} phenotypes in the discovery and replication cohorts.

	Discovery Cohort			**Replication Cohort**				
	IRF7^{hi}	IRF7^{lo}	Hi vs Lo	IRF7^{hi}	IRF7^{low1}	Hi vs Low1	IRF7^{low2}	Hi vs Low2
N	26	19	p-value	49	29	p-value	21	p-value
Age, mean (SD), yrs	4.73 (3.34), n=26	3.65 (2.85), n=19	0.26	4.99 (3.51), n=49	5.85 (3.29), n=29	0.285	6.05 (4.27), n=21	0.28
Male Gender, n/N (%)	14/26 (53.8)	10/19 (52.6)	1	27/49 (55.1)	23/29 (79.3)	**0.05**	12/21 (57.1)	1
Caucasian, n/N (%)	10/26 (38.5)	11/19 (57.9)	0.237	23/48 (47.9)	11/28 (39.3)	0.485	13/20 (65.0)	0.287
Spring recruitment, n/N (%)	3/26 (11.5)	1/19 (5.3)	0.627	13/49 (26.5)	7/29 (24.1)	1	7/21 (33.3)	0.576
Autumn recruitment, n/N (%)	4/26 (15.4)	2/19 (10.5)	1	10/49 (20.4)	12/29 (41.4)	0.068	6/21 (28.6)	0.538
Winter recruitment, n/N (%)	19/26 (73.1)	16/19 (84.2)	0.481	25/49 (51.0)	10/29 (34.5)	0.168	7/21 (33.3)	0.2
Overall Allergy, n/N (%)	20/26 (76.9)	8/19 (42.1)	**0.029**	37/49 (75.5)	25/29 (86.2)	0.385	16/21 (76.2)	1
AeroAllergy, n/N (%)	19/26 (73.1)	6/19 (31.6)	**0.008**	31/49 (63.3)	23/29 (79.3)	0.204	16/21 (76.2)	0.407
Pathogen Detection								
Respiratory virus+, n/N (%)	22/26 (84.6)	16/17 (94.1)	0.633	38/47 (80.9)	16/26 (61.5)	0.096	18/20 (90.0)	0.484
RV+, n/N (%)	19/26 (73.1)	11/19 (57.9)	0.347	32/47 (68.1)	16/29 (55.2)	0.329	16/21 (76.2)	0.575
RVC+, n/N (%)	14/26 (53.8)	7/19 (36.8)	0.366	19/46 (41.3)	11/28 (39.3)	1	11/19 (57.9)	0.279
RVA+, n/N (%)	5/26 (19.2)	4/19 (21.1)	1	9/46 (19.6)	4/28 (14.3)	0.755	3/19 (15.8)	1
RSV+, n/N (%)	1/25 (4.0)	4/17 (23.5)	0.14	6/43 (14.0)	0/25 (0)	0.078	1/16 (6.3)	0.661
No. of Virus+, mean (SD)	1.20 (0.87) n=25	1.17 (0.58), n=12	0.905	0.98 (0.72), n=41	0.64 (0.57), n=25	0.053	0.87 (0.35), n=15	0.58
Bacteria+, n/N (%)	18/25 (72.0)	9/12 (75.0)	1	23/39 (59.0)	10/23 (43.5)	0.296	7/13 (53.8)	0.757
No. of Bacteria+, mean (SD)	1.12 (0.93), n=25	1.08 (0.79), n=12	0.907	0.80 (0.78), n=41	0.52 (0.71), n=25	0.143	0.75 (0.86), n=15	0.817
No. of virus+ and bacteria+, mean (SD)	2.32 (1.41), n=25	2.25 (1.14), n=12	0.882	1.78 (1.15), n=41	1.16 (0.99), n=25	**0.029**	1.60 (0.91), n=15	0.587

Symptoms Prior to Presentation to Hospital

Symptoms of URTI, n/N (%)	23/26 (88.5)	18/19 (94.7)	0.627	45/49 (91.8)	23/29 (79.3)	0.161	14/20 (70.0)	**0.029**
Time from first symptom to hospital presentation, mean (SD), days	2.31 (1.98), n=26	4.74 (4.03), n=19	**0.011**	2.20 (1.76), n=49	3.90 (4.59), n=29	**0.023**	1.90 (1.80), n=20	0.519
Time from first symptom to recruitment, mean (SD), days	2.85 (2.0), n=26	5.74 (4.16), n=19	**0.003**	3.102 (1.82), n=49	4.59 (4.84), n=29	0.057	2.80 (1.94), n=20	0.541
Severity zscore, mean (SD)	0.67 (0.74), n=24	0.42 (0.76), n=18	0.284	0.45 (0.93), n=41	0.71 (0.55), n=25	0.205	0.65 (0.66), n=21	0.374
Cough, n/N (%)	20/25 (80)	18/18 (100)	0.064	44/49 (89.8)	28/28 (100)	0.152	19/20 (95.0)	0.664
Cough duration, mean (SD), days	1.96 (1.51), n=25	5.62 (3.20), n=13	**<0.001**	2.00 (1.17), n=45	3.75 (4.44), n=24	**0.015**	2.25 (1.77), n=20	0.502
Wheeze, n/N (%)	26/26 (100)	16/19 (84.2)	0.068	48/49 (98.0)	28/29 (96.6)	1	19/20 (95.0)	0.499
Wheeze duration, mean (SD), days	1.69 (.84), n=26	2.35 (1.77), n=17	0.106	1.74 (0.99), n=47	3.56 (5.15), n=27	**0.022**	1.85 (1.14), n=20	0.704
Short of breath, n/N (%)	26/26 (100)	16/19 (84.2)	0.068	47/49 (95.9)	27/29 (93.1)	0.625	18/20 (90.0)	0.574
Short of breath duration, mean (SD), days	1.62 (0.80), n=26	2.18 (1.51), n=17	0.12	1.61 (0.95), n=46	3.41 (5.00), n=29	**0.02**	1.70 (1.17), n=20	0.74
Fever, n/N (%)	10/26 (38.5)	9/19 (47.4)	0.761	29/49 (59.2)	7/29 (24.1)	**0.004**	2/20 (10.0)	**<0.001**
Fever duration, mean (SD), days	0.88 (1.58), n=26	1.39 (2.09), n=18	0.368	1.22 (1.34), n=49	0.64 (1.50), n=28	0.084	0.20 (0.70), n=20	**0.002**
Weak and tired, n/N (%)	8/26 (30.8)	13/19 (68.4)	**0.017**	29/49 (59.2)	17/29 (58.6)	1	9/20 (45.0)	0.301
Weak and tired duration, mean (SD), days	1.23 (2.23), n=26	2.24 (2.33), n=17	0.164	1.38 (1.55), n=48	2.22 (4.07), n=27	0.201	1.05 (1.50), n=20	0.43
Runny nose, n/N (%)	17/26 (65.4)	15/19 (78.9)	0.507	37/49 (75.5)	19/29 (65.5)	0.436	9/20 (45.0)	**0.024**
Runny nose duration, mean (SD), days	2.12 (2.22), n=25	3.94 (4.49), n=17	0.089	2.52 (3.38), n=48	2.41 (3.02), n=29	0.889	1.40 (2.06), n=20	0.174
Congestion, n/N (%)	10/25 (40.0)	9/19 (47.4)	0.761	21/49 (42.9)	10/29 (34.5)	0.485	5/20 (25.0)	0.185
Congestion duration, mean (SD), days	1.24 (1.86), n=25	3.00 (4.76), n=18	0.1	1.63 (3.47), n=49	1.41 (2.90), n=29	0.776	0.95 (2.01), n=20	0.413
Sneeze, n/N (%)	9/25 (36.0)	12/19 (63.2)	0.127	25/49 (51.0)	14/29 (48.3)	1	9/20 (45.0)	0.792

Sneeze duration, mean (SD), days	1.40 (2.24), n=25	3.31 (4.88), n=16	0.096	1.85 (3.50), n=47	1.46 (1.99), n=28	0.595	1.20 (1.96), n=20	0.439
Sore throat, n/N (%)	2/26 (7.7)	0 (0)	0.501	0/49 (0)	1/29 (3.4)	0.372	1/21 (4.8)	0.3
Hospital Admission and Medication								
Admission to hospital, n/N (%)	7/26 (26.9)	12/19 (63.2)	**0.031**	22/49 (44.9)	12/29 (41.4)	0.816	8/21 (38.1)	0.793
Time from presentation to recruitment, mean (SD), days	0.85 (0.61), n=26	0.74 (0.73), n=19	0.589	0.90 (0.71), n=49	0.69 (0.71), n=29	0.217	0.90 (0.72), n=20	0.991
Time to discharge, mean (SD), hr	27.64 (16.06), n=26	39.07 (29.07), n=18	0.102	29.83 (26.67), n=48	35.28 (45.78), n=29	0.511	40.95 (36.97), n=21	0.163
Steroid, n/N (%)	16/17 (94.1)	12/14 (85.7)	0.576	32/45 (71.1)	21/28 (75.0)	0.792	15/17 (83.2)	0.2
Time from steroid to sample collection, mean (SD), hr	6.31 (5.20), n=16	11.77 (14.25), n=10	0.174	7.61 (6.33), n=24	11.34 (14.97), n=17	0.28	7.47 (6.36), n=14	0.947
Antibiotics, n/N (%)	3/21 (14.3)	3/15 (20.0)	0.677	10/45 (22.2)	7/26 (26.9)	0.774	2/19 (10.5)	0.484
No. of Vent doses in 6hr	7.39 (3.55), n=23	6.17 (3.35), n=12	0.331	7.37 (3.35), n=43	7.74 (3.43), n=27	0.658	8.48 (5.69), n=21	0.332
No. of Vent doses in 12hr	10.43 (5.03), n=23	9.33 (5.24), n=12	0.548	10.58 (6.11), n=43	10.59 (5.28), n=27	0.994	12.29 (6.77), n=21	0.316
No. of Vent doses in 24hr	13.57 (7.43), n=23	10.50 (5.70), n=12	0.221	14.46 (10.79), n=43	14.26 (7.73), n=27	0.932	18.19 (9.10), n=21	0.178
First Respiratory Representation								
Time to first respiratory representation to hospital within the first 12 months of follow-up, median, days	>365	225	**0.015**	>365	>365	0.682	>365	0.57
No. of children represented within the first 12 months of follow-up, n/N (%)	8/26 (30.8)	13/19 (68.4)	**0.017**	19/48 (39.6)	10/29 (34.5)	0.809	7/21 (33.3)	0.788

Time to first respiratory representation to hospital within the first 24 months of follow-up, median, days	>730	225	**0.05**
No. of children represented within the first 24 months of follow-up, n/N (%)	11/26 (42.3)	13/19 (68.4)	0.131

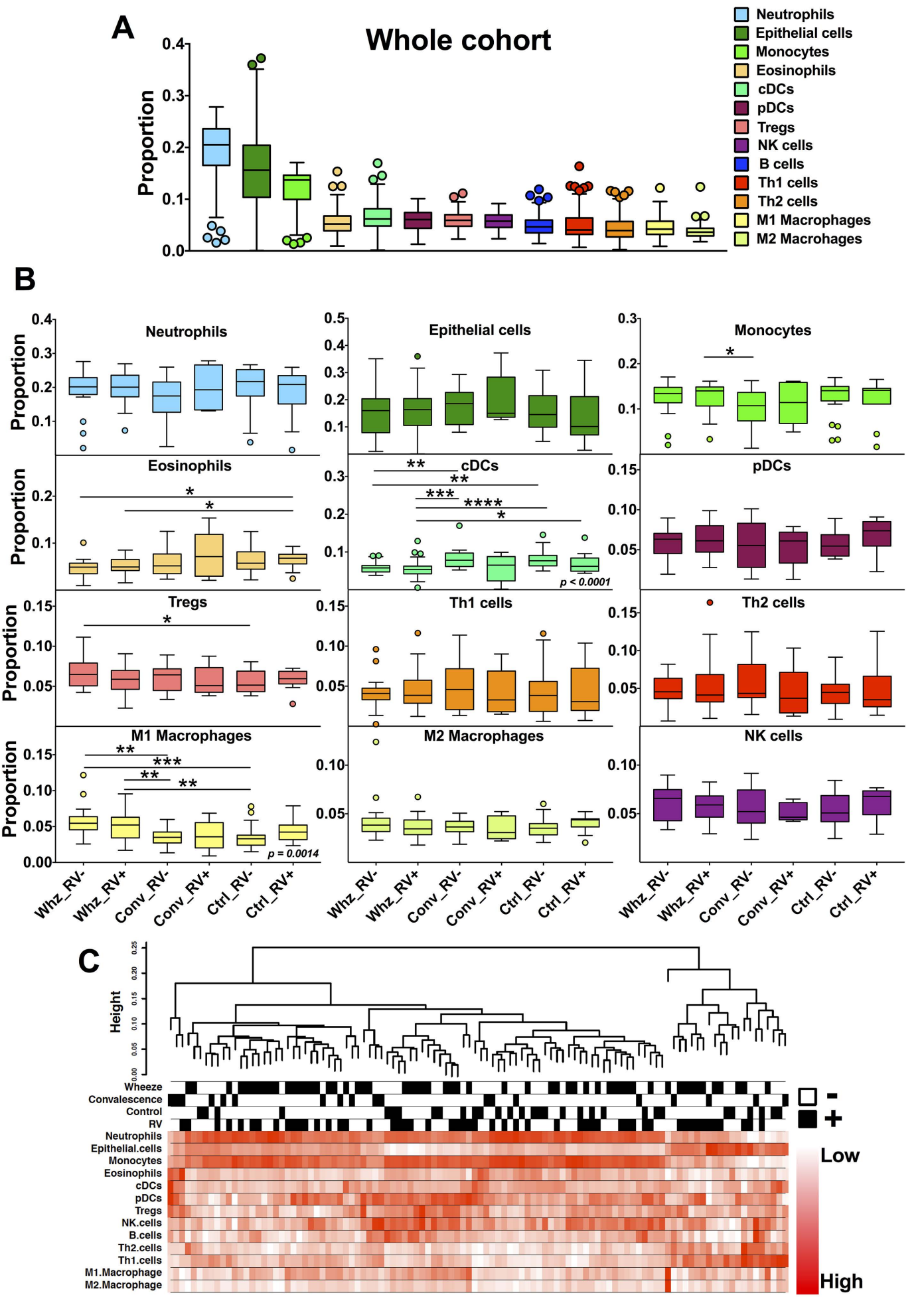
A
Whole cohort
Proportion
Neutrophils
Epithelial cells
Monocytes
Eosinophils
cDCs
pDCs
Tregs
NK cells
B cells
Th1 cells
Th2 cells
M1 Macrophages
M2 Macrohages
B
Neutrophils
Epithelial cells
Monocytes
Eosinophils
cDCs
pDCs
Tregs
Th1 cells
Th2 cells
M1 Macrophages
M2 Macrophages
NK cells
p < 0.0001
p = 0.0014
Whz_RV-
Whz_RV+
Conv_RV-
Conv_RV+
Ctrl_RV-
Ctrl_RV+
C
Height
Wheeze
Convalescence
Control
RV
Neutrophils
Epithelial.cells
Monocytes
Eosinophils
cDCs
pDCs
Tregs
NK.cells
B.cells
Th2.cells
Th1.cells
M1.Macrophage
M2.Macrophage
Low
High

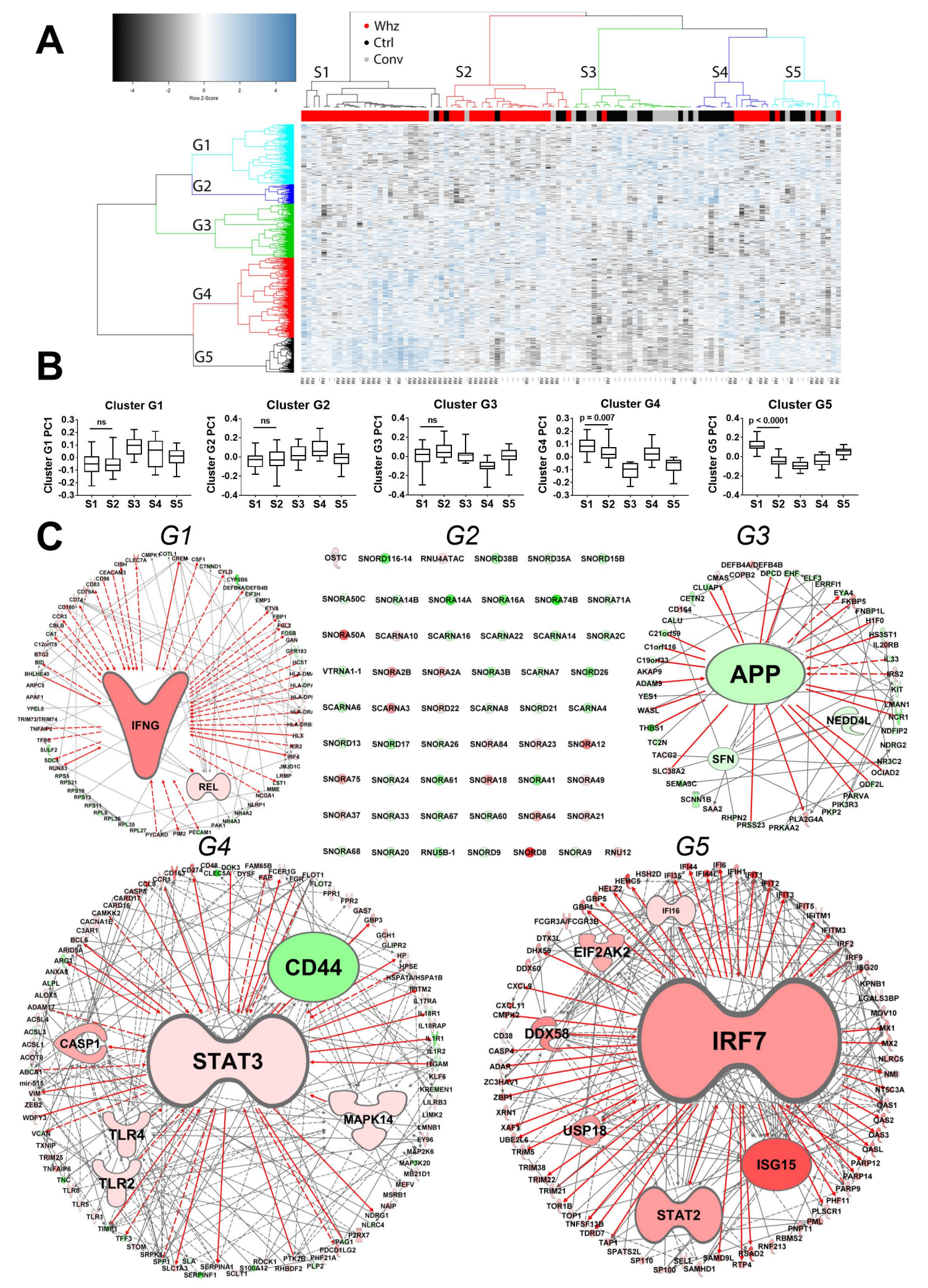
A
Whz
Ctrl
Conv
S1
S2
S3
S4
S5
G1
G2
G3
G4
G5
Row Z-Score
B
Cluster G1
Cluster G2
Cluster G3
Cluster G4
Cluster G5
Cluster G1 PC1
Cluster G2 PC1
Cluster G3 PC1
Cluster G4 PC1
Cluster G5 PC1
ns
p = 0.007
p < 0.0001
C
G1
G2
G3
G4
G5
IFNG
REL
APP
NEDD4L
SFN
CD44
STAT3
CASP1
MAPK14
TLR4
TLR2
IRF7
EIF2AK2
DDX58
USP18
ISG15
STAT2
OSTC
SNORD116-14
RNU4ATAC
SNORD38B
SNORD35A
SNORD15B
SNORA50C
SNORA14B
SNORA14A
SNORA16A
SNORA74B
SNORA71A
SNORA50A
SCARNA10
SCARNA16
SCARNA22
SCARNA14
SNORA2C
VTRNA1-1
SNORA2B
SNORA2A
SNORA3B
SCARNA7
SNORD26
SCARNA6
SCARNA3
SNORD22
SCARNA8
SNORD21
SCARNA4
SNORD13
SNORD17
SNORA26
SNORA84
SNORA23
SNORA12
SNORA75
SNORA24
SNORA61
SNORA18
SNORA41
SNORA49
SNORA37
SNORA33
SNORA67
SNORA60
SNORA64
SNORA21
SNORA68
SNORA20
RNU5B-1
SNORD9
SNORD8
SNORA9
RNU12

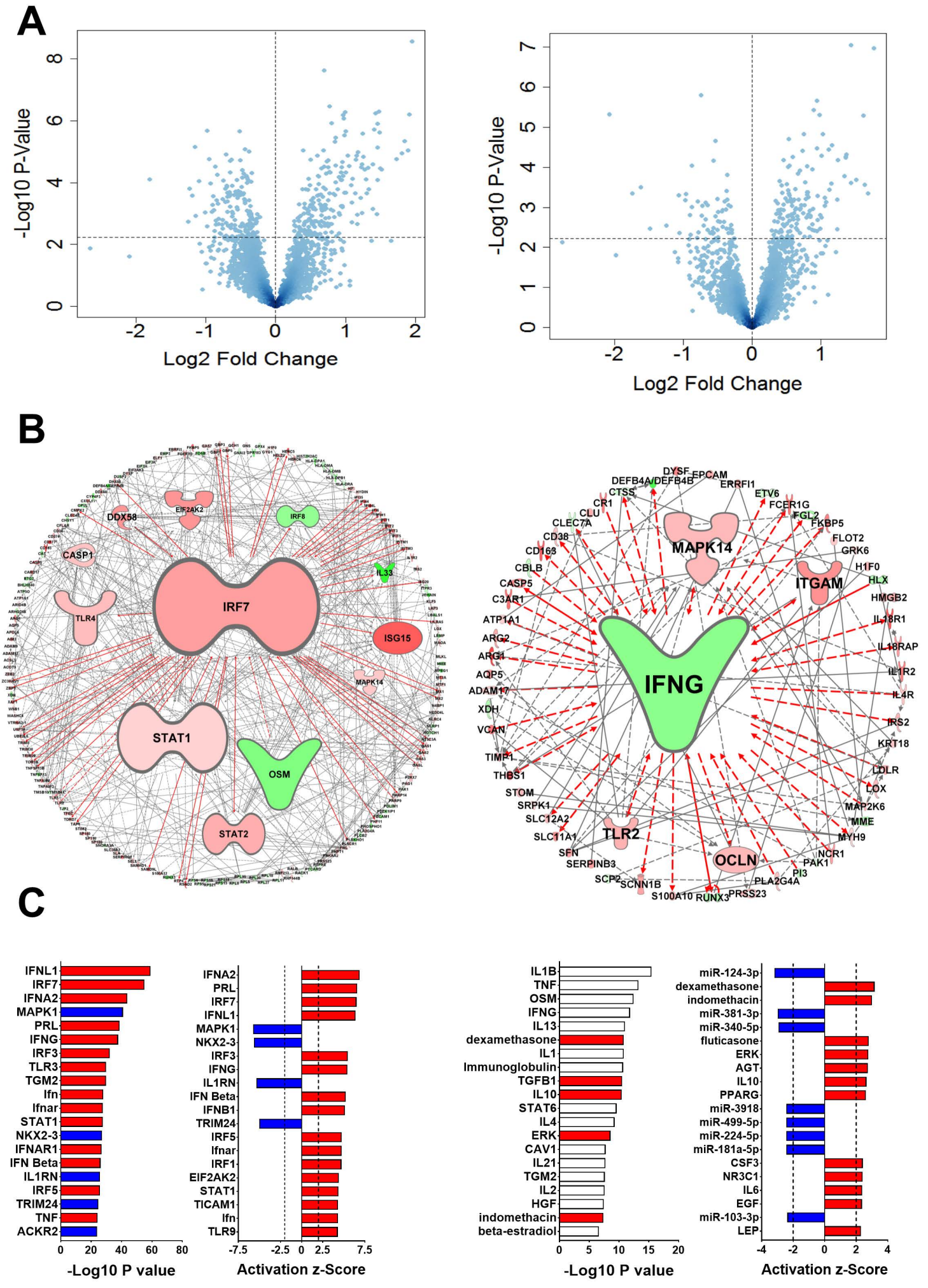
A
-Log10 P-Value
Log2 Fold Change
-Log10 P-Value
Log2 Fold Change
B
DDX58
EIF2AK2
IRF8
CASP1
IL33
IRF7
TLR4
ISG15
MAPK14
STAT1
OSM
STAT2
MAPK14
ITGAM
IFNG
TLR2
OCLN
C
IFNL1
IRF7
IFNA2
MAPK1
PRL
IFNG
IRF3
TLR3
TGM2
Ifn
Ifnar
STAT1
NKX2-3
IFNAR1
IFN Beta
IL1RN
IRF5
TRIM24
TNF
ACKR2
-Log10 P value
IFNA2
PRL
IRF7
IFNL1
MAPK1
NKX2-3
IRF3
IFNG
IL1RN
IFN Beta
IFNB1
TRIM24
IRF5
Ifnar
IRF1
EIF2AK2
STAT1
TICAM1
Ifn
TLR9
Activation z-Score
IL1B
TNF
OSM
IFNG
IL13
dexamethasone
IL1
Immunoglobulin
TGFB1
IL10
STAT6
IL4
ERK
CAV1
IL21
TGM2
IL2
HGF
indomethacin
beta-estradiol
-Log10 P value
miR-124-3p
dexamethasone
indomethacin
miR-381-3p
miR-340-5p
fluticasone
ERK
AGT
IL10
PPARG
miR-3918
miR-499-5p
miR-224-5p
miR-181a-5p
CSF3
NR3C1
IL6
EGF
miR-103-3p
LEP
Activation z-Score

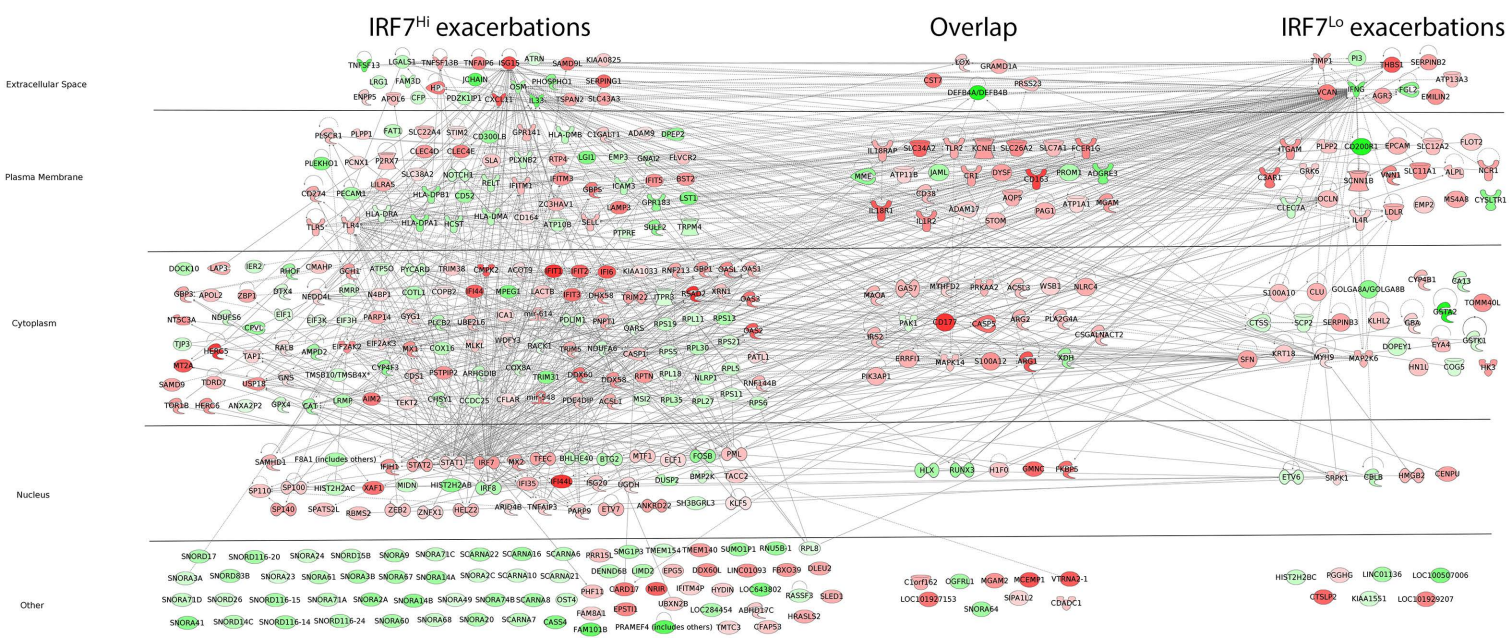
IRF7Hi exacerbations
Overlap
IRF7Lo exacerbations
Extracellular Space
Plasma Membrane
Cytoplasm
Nucleus
Other

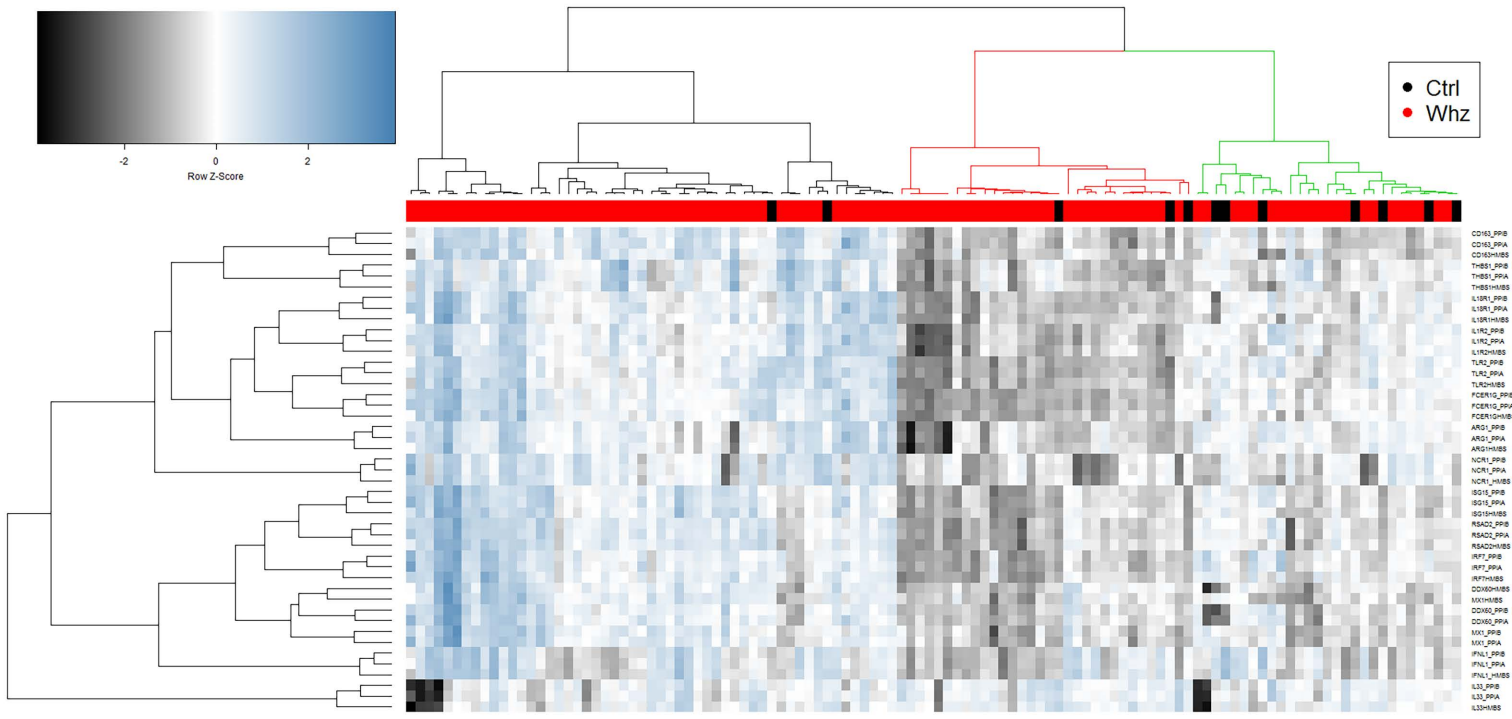
-2
0
2
Row Z-Score
Ctrl
Whz
CD163_PPIB
CD163_PPIA
CD163+M/BS
THBS1_PPIB
THBS1_PPIA
THBS1+M/BS
IL1R1_PPIB
IL1R1_PPIA
IL1R1+M/BS
IL1R2_PPIB
IL1R2_PPIA
IL1R2+M/BS
TLR2_PPIB
TLR2_PPIA
TLR2+M/BS
FCER1G_PPIB
FCER1G_PPIA
FCER1G+M/BS
ARG1_PPIB
ARG1_PPIA
ARG1+M/BS
NCR1_PPIB
NCR1_PPIA
NCR1_+M/BS
ISG15_PPIB
ISG15_PPIA
ISG15+M/BS
RSAD2_PPIB
RSAD2_PPIA
RSAD2+M/BS
IRF7_PPIB
IRF7_PPIA
IRF7+M/BS
DDX60+M/BS
MX1+M/BS
DDX60_PPIB
DDX60_PPIA
MX1_PPIB
MX1_PPIA
IFNL1_PPIB
IFNL1_PPIA
IFNL1_+M/BS
IL33_PPIB
IL33_PPIA
IL33+M/BS